

Disorder Driven Melting of the Vortex Line Lattice

P. Olsson¹ and S. Teitel²

¹*Department of Theoretical Physics, Umeå University, 901 87 Umeå Sweden*

²*Department of Physics and Astronomy, University of Rochester, Rochester, NY 14627*

(October 27, 2018)

We use Monte Carlo simulations of the 3D uniformly frustrated XY model, with uncorrelated quenched randomness in the in-plane couplings, to model the effect of random point pins on the vortex line phases of a type II superconductor. We map out the phase diagram as a function of temperature T and randomness strength p for fixed applied magnetic field. We find that, as p increases to a critical value p_c , the first order vortex lattice melting line turns parallel to the T axis, and continues smoothly down to low temperature, rather than ending at a critical point. The entropy jump across this line at p_c vanishes, but the transition remains first order. Above this disorder driven transition line, we find that the helicity modulus parallel to the applied field vanishes, and so no true phase coherent vortex glass exists.

74.60.Ge, 64.60-i, 74.76-w

Experimental [1–3], theoretical [4–6] and numerical [7,8] studies have argued that the effect of intrinsic point impurities on otherwise clean single crystal samples of high T_c superconductors leads to a $H - T$ phase diagram with the following generic form. At low magnetic fields H , an elastically distorted vortex lattice (the “Bragg glass” [4]) undergoes a first order melting transition to a vortex liquid as temperature T is increased. This melting line $T_c(H)$ continues as H is increased, until an “upper critical point,” T_{ucp} , is reached above which sharp discontinuities in measured quantities become smeared. Upon increasing H at lower temperatures, $T < T_{ucp}$, the vortex lattice undergoes a transformation to a disordered vortex state along a line, $H_{sp}(T)$, characterized by the “second magnetization peak” where critical currents show a sharp increase. As T increases, the $H_{sp}(T)$ line continues to the vicinity of T_{ucp} . In BSCCO, $H_{sp}(T)$ is only weakly dependent on T [2]. Very recently, several experiments [9] have provided strong evidence that the $H_{sp}(T)$ line in BSCCO is associated with a thermodynamic first order phase transition. Whether the disordered state above $H_{sp}(T)$ is a “vortex glass” [5], characterized by true superconducting phase coherence and separated from the vortex liquid by a sharp phase transition, or whether it is a dynamically frozen state that smoothly crosses over to the vortex liquid, remains a topic of controversy [10].

Since many of the experimental and numerical studies focus on dynamical probes, from which it can sometimes be difficult to infer a true equilibrium phase transition, and analytical models must resort to Lindemann or other simplifying approximations, it is important to establish the true equilibrium phase diagram within a realistic model system. Towards this end we have carried out extensive Monte Carlo (MC) studies of the uniformly frustrated three dimensional (3D) XY model [11], with uncorrelated quenched random couplings to model point impurities. Applying a fixed magnetic field B we map out the phase diagram as a function of disorder strength

p and temperature T . Increasing p at fixed B is believed to play a similar role as the more physical case of increasing B at fixed p . Taking great care to achieve proper equilibration, and measuring thermodynamic derivatives of the free energy, we find in our model a single first order phase boundary. At small p , the transition, $T_c(p)$, is a thermally driven melting of the vortex lattice. Increasing p , there is a maximum critical p_c above which disorder destroys the vortex lattice; when $p = p_c$, the transition line $T_c(p)$ turns parallel to the T axis and smoothly continues down to low T . No critical point is found to separate the thermal from the disorder driven sections of the phase boundary. For $p > p_c$ we find no evidence for a true phase coherent vortex glass.

The model we study is given by the Hamiltonian

$$\mathcal{H}[\theta_i] = - \sum_{\text{bonds } i\mu} J_{i\mu} \cos(\theta_i - \theta_{i+\hat{\mu}} - A_{i\mu}) \quad (1)$$

where θ_i is the phase of the superconducting wavefunction on site i of a 3D periodic cubic grid of sites, the sum is over all bonds in directions $\hat{\mu} = \hat{x}, \hat{y}, \hat{z}$, and $A_{i\mu} = (2\pi/\phi_0) \int_i^{i+\hat{\mu}} \mathbf{A} \cdot d\mathbf{l}$ is the integral of the magnetic vector potential across bond $i\mu$, where $\nabla \times \mathbf{A} = B\hat{z}$ is a fixed uniform magnetic field in the \hat{z} direction. To model uncorrelated random point vortex pinning in the xy planes, we take,

$$\begin{aligned} J_{i\mu} &= J_z, & \mu &= z \\ J_{i\mu} &= J_{\perp}(1 + p\epsilon_{i\mu}), & \mu &= x, y \end{aligned} \quad (2)$$

The coupling between planes J_z is uniform, while each bond in the xy plane is randomly perturbed about the constant value J_{\perp} ; the $\epsilon_{i\mu}$ are independent Gaussian random variables with $\langle \epsilon_{i\mu} \rangle = 0$, $\langle \epsilon_{i\mu}^2 \rangle = 1$. The parameter p controls the strength of the disorder. For computational convenience we choose $J_z/J_{\perp} = 1/40$, with a vortex line density of $f = a_{\perp}^2 B/\phi_0 = 1/20$, where a_{\perp} is the grid spacing in the xy plane, and $\phi_0 = hc/2e$ is the flux quantum.

Our system size is $L_x = L_y = 40$, with $L_z = 16$. To check finite size effects, we have also considered $L_z = 24$ and 32 for certain cases. Our runs are typically $1 - 10 \times 10^7$ MC sweeps through the entire lattice near transitions. Our results below are for a single realization of the disorder only. The extremely time consuming nature of our simulations excluded any serious attempt at disorder averaging. We have, however, carried out similar analyses for two other realizations of the disorder and have found qualitatively the same behavior.

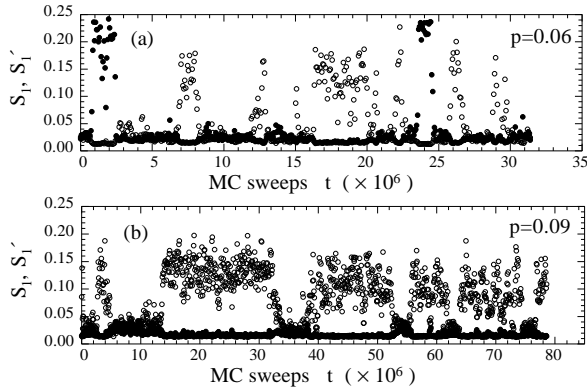


FIG. 1. S_1 (\bullet) and S'_1 (\circ) vs. number of Monte Carlo sweeps t for disorder strengths (a) $p = 0.06$, $T_c = 0.255$, and (b) $p = 0.09$, $T_c = 0.200$. The system width is $L_z = 16$. Each data point is an average over 2^{16} sweeps.

In the pure model, $p = 0$, the low temperature vortex line lattice has a first order melting transition to a vortex line liquid [12]. To map out this melting transition line in the $p-T$ plane we fix the disorder strength p , and cool down from high T , until we reach a temperature $T_c(p)$ at which we observe repeated hopping back and forth between coexisting vortex liquid and lattice phases. To detect the vortex lattice, we measure the in-plane vortex structure function (normalized for convenience so that $S(0) = 1$),

$$S(\mathbf{k}_\perp) = \frac{1}{f^2 N} \sum_{\mathbf{r}_\perp, z} \langle n_z(\mathbf{r}_\perp, z) n_z(0, z) \rangle e^{i\mathbf{k}_\perp \cdot \mathbf{r}_\perp} \quad (3)$$

where n_z is the vorticity in the xy plane, and $N = L_x L_y L_z$. $S(\mathbf{k}_\perp)$ will have Bragg peaks at the reciprocal lattice vectors $\{\mathbf{K}\}$ of the vortex lattice. We find that the vortex lattice always orders into the same periodicity as that of the pure $p = 0$ case, where there are two possible lattice orientations related by a 90° rotation. Defining S_1 as the average of $S(\mathbf{K})$ over the six smallest non-zero $\{\mathbf{K}\}$ for one lattice orientation, and S'_1 as that for the other orientation, we identify the vortex lattice as states in which either S_1 or S'_1 is large, according to which of the two lattice orientations has formed; in contrast, in the vortex liquid, both S_1 and S'_1 are small. In Fig. 1 we plot S_1 and S'_1 vs. MC simulation time t at $T_c(p)$ for two disorder strengths. For the weaker disorder, $p = 0.06$, we see both orientations of lattice coexisting with the liq-

uid. For the stronger $p = 0.09$, the disorder sufficiently breaks the degeneracy of the two lattice orientations, so that we see only coexistence between one particular lattice orientation and the liquid. The repeated hopping between lattice and liquid in Fig. 1 verifies that we are well equilibrated. In this manner, by varying p , we determine the melting phase boundary $T_c(p)$ shown in Fig. 2. We include in Fig. 2 several data points for systems with $L_z = 24$, showing only a small shift in the phase boundary as L_z increased.

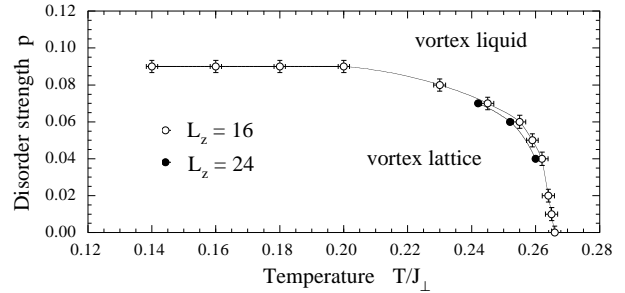


FIG. 2. Vortex lattice melting phase boundary in the $p-T$ plane, for $L_z = 16$ (\circ) and $L_z = 24$ (\bullet).

We now determine if the melting transition $T_c(p)$ remains 1st order, as p increases. First order transitions are characterized by discontinuous jumps in thermodynamic quantities. Here we consider the average energy per site E (the conjugate variable to temperature T), and a variable Q defined to be conjugate to the disorder strength p ,

$$E = -\frac{1}{N} \sum_{i\mu} J_{i\mu} \langle \cos(\theta_i - \theta_{i+\hat{\mu}} - A_{i\mu}) \rangle \quad (4)$$

$$Q \equiv \frac{1}{N} \frac{\partial F}{\partial p} = -\frac{J_\perp}{N} \sum_{i, \mu=x, y} \epsilon_{i\mu} \langle \cos(\theta_i - \theta_{i+\hat{\mu}} - A_{i\mu}) \rangle, \quad (5)$$

where F is the total free energy.

To see if there is a discrete jump in E or Q at $T_c(p)$, we use the values of S_1 and S'_1 to sort microscopic states as either vortex lattice or liquid. We can then compute the properties of each phase separately. In Figs. 3a and 3b we show semilog plots of the histograms $P(\Delta S_1)$ of values of $\Delta S_1 \equiv S_1 - S'_1$ encountered during our simulation at $T_c(p)$, for the two cases of Fig. 1. In Fig. 3a, for $p = 0.06$, we see separated peaks for the liquid at $\Delta S_1 = 0$, and for the two lattice orientations at finite positive and negative values of ΔS_1 . In Fig. 3b, for the stronger $p = 0.09$, we see only peaks for the liquid and one of the two lattice orientations. Fitting these peaks to empirical forms (Gaussian for the lattice, exponential for the liquid; these are the solid lines in Figs. 3a,b), we determine the relative probability for a state with a given value of ΔS_1 to belong to the liquid phase, or either of the two orientations of the lattice phases. Sorting through our microscopic states we probabilistically assign each to one of these three phases. We then plot the histograms

of E and Q values separately for each phase.

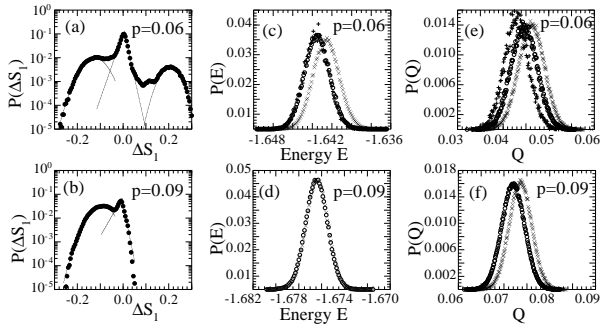


FIG. 3. Histograms of $\Delta S_1 \equiv S_1 - S'_1$, energy E , and disorder conjugate Q for $p = 0.06$, $T_c = 0.255$ and $p = 0.09$, $T_c = 0.200$, for $L_z = 16$, at the melting temperature $T_c(p)$. (o) and (+) are for the two lattice orientations, (x) are for the liquid.

In Fig. 3c we show the histograms $P(E)$ for $p = 0.06$. While the two lattice orientations have the same energy distribution, there is a clear difference between the liquid and lattice. This results in a finite energy jump ΔE , and hence a finite entropy jump $\Delta E/T$, between the liquid and lattice. The melting transition is clearly first order. The histograms $P(Q)$ for $p = 0.06$ are shown in Fig. 3e, where we also see a finite jump ΔQ between liquid and lattice; for Q the disorder also couples differently to the two lattice orientations.

In Fig. 3d we show the histograms $P(E)$ for the more strongly disordered $p = 0.09$, where only one lattice orientation is found. In contrast to Fig. 3c, we find that the energy distributions of the liquid and the lattice are now *identical!* Thus there is no energy jump, and hence no entropy jump, and moreover no specific heat jump, in going from liquid to lattice. However the histograms of $P(Q)$ plotted in Fig. 3f remain clearly different for liquid and lattice, and so there remains a finite jump ΔQ at the melting transition. The transition at $p = 0.09$ therefore remains first order, even though the entropy jump has vanished. Combining $\Delta E = 0$ with the Clausius-Clapeyron relation, we conclude that the melting line must now be perfectly parallel to the temperature axis [13], and the transition becomes disorder, rather than thermally, driven. As shown in Fig. 2, we have been able to follow the melting line from where it first turns parallel to the T axis, down to several lower temperatures.

In Fig. 4 we plot ΔE and ΔQ vs. p along the melting line. That ΔE and ΔQ never simultaneously vanish, indicates that no critical point exists along the melting line.

Although our simulations are for a specific fixed value of B , if we assume that the above result continues to hold for general values of B , then it must be true that the phase diagram in the $B-T$ plane at fixed p must similarly turn parallel to the T axis at low temperatures. The point where the melting line first turns parallel to the T

axis has many features in common with an “upper critical point”; discontinuities as T varies across the melting line below this point, will cease to exist as T varies above this point. Yet there is no true critical end point and the first order melting line extends continuously down to lower temperatures.

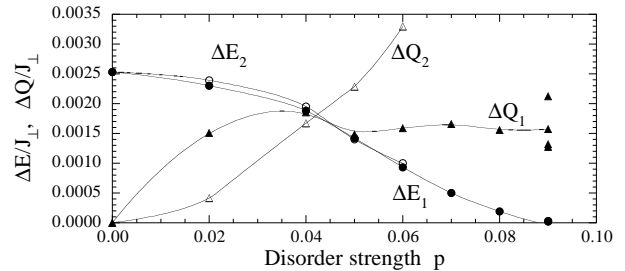


FIG. 4. Jumps ΔE and ΔQ , vs. p , along the melting line, $T_c(p)$, for $L_z = 16$. Subscripts “1” and “2” refer to the two possible orientations of the vortex lattice (solid and open symbols respectively).

Next, we investigate the superconducting phase coherence in our model, by computing the helicity modulus [11], Υ_z , parallel to the applied magnetic field. $\Upsilon_z = 0$ indicates the absence of phase coherence. In Fig. 5a we show Υ_z vs. T , for two different disorder strengths $p < p_c = 0.09$, comparing systems with $L_z = 16$ and $L_z = 24$. In both cases we see a discontinuous jump in Υ_z at the melting transition (at T_c we compute Υ_z separately for the coexisting lattice and liquid phases, using the decomposition of our states according to ΔS_1). As L_z is increased, we see that Υ_z vanishes in the vortex liquid; the vortex lattice melting thus marks the loss of superconducting phase coherence.

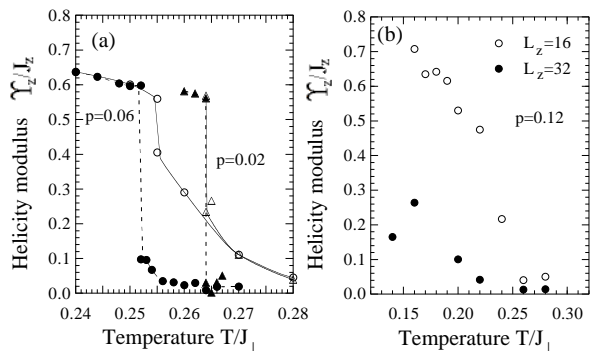


FIG. 5. Longitudinal helicity modulus Υ_z/J_z vs. T for disorder strengths (a) $p = 0.02$ and $p = 0.06 < p_c$ (open symbols and solid lines are for $L_z = 16$; solid symbols and dashed lines are for $L_z = 24$) and (b) $p = 0.12 > p_c$.

We now consider $p > p_c$ to see if a phase coherent vortex glass state might exist above the disorder driven melting of the vortex lattice. In Fig. 5b we show Υ_z vs. T for $p = 0.12$ and system sizes $L_z = 16$ and $L_z = 32$. Although it becomes extremely difficult to equilibrate

our $L_z = 32$ system at such low T , we see a dramatic finite size effect strongly suggesting that Υ_z decreases to zero as L_z increases. We therefore find no evidence for a true phase coherent vortex glass. Our result agrees with conclusions from dynamical simulations of an interacting vortex line model by Reichhardt *et al* [8]. In contrast, recent work by Kawamura [14] found a finite vortex glass T_c in numerical studies of a model similar to Eq.(1), but at a higher field density $f = 1/2\pi$ and J_{ij} uniformly distributed on $[0, 2]$. It is not clear if this disagreement is due his much stronger random pin strengths, or possible finite size effects in his systems of $L \leq 16$. A vortex glass transition has also recently been found for an interacting vortex line model with $f = 1/2$ and very strong pinning [15].

Finally, in Fig. 6 we plot the longitudinal phase angle correlation length, ξ_z , in the liquid $T \geq T_c(p)$, as determined by fitting the correlation function,

$$C(z) = \sum_j \langle e^{i[\theta_j - \theta_{j+z}]} \rangle, \quad (6)$$

to an exponential decay for $z < L_z/2$. We see that for fixed T , ξ_z decreases as p increases. However, since $T_c(p)$ decreases as p increases, the value $\xi_z(T_c(p))$ at melting *increases* as p increases. Even in the disordered state above p_c we find that ξ_z can be as large as in the liquid just above the thermally driven melting line. This suggests that the disorder driven melting should not be thought of as a layer decoupling transition.

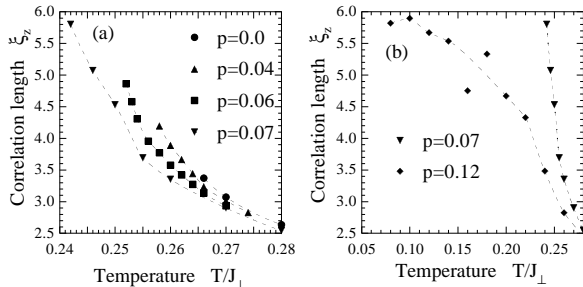


FIG. 6. Longitudinal correlation length ξ_z vs. T in the vortex liquid phase for (a) several values of disorder $p < p_c = 0.09$ at $L_z = 24$; and for (b) $p = 0.12 > p_c$ at $L_z = 32$, in comparison to $p = 0.07 < p_c$ from (a).

As we were finishing this work, we learned of similar work by Nonomura and Hu [16], using the same model (1) with a slightly different scheme for the point randomness and a much weaker inter-planar coupling, $J_z/J_{\perp} = 1/400$. Using different methods they too find a disorder driven 1st order vortex lattice melting line nearly parallel to the T axis at low T . However they also claim to find a 1st order “vortex slush” to liquid transition extending to higher disorder from the thermally driven melting line, as well as a vortex glass to vortex slush transition at lower T . We too find a peak in specific heat for $p > p_c$ that lies at a T in the vicinity of

the thermally driven melting line, however we have interpreted this as a smooth crossover rather than a true phase transition.

We would like to thank C. Marcenat for a valuable discussion. This work was supported by the Engineering Research Program of the Office of Basic Energy Sciences at the Department of Energy grant DE-FG02-89ER14017, the Swedish Natural Science Research Council Contract No. E 5106-1643/1999, and by the resources of the Swedish High Performance Computing Center North (HPC2N). Travel between Rochester and Umeå was supported by grants NSF INT-9901379 and STINT 99/976(00).

-
- [1] R. Cubitt *et al.* Nature **365**, 407 (1993).
 - [2] B. Khayhovich *et al.*, Phys. Rev. Lett. **76**, 2555 (1996), Phys. Rev. B **56**, R517 (1997).
 - [3] T. Nishizaki *et al.*, Phys. Rev. B **61**, 3649 (2000).
 - [4] T. Giamarchi and P. Le Doussal, Phys. Rev. Lett. **72**, 1530 (1994) and Phys. Rev. B **52**, 1242 (1995); T. Nattermann, Phys. Rev. Lett. **64**, 2454 (1990); D.S. Fisher, Phys. Rev. Lett. **78**, 1964 (1997); T. Nattermann and S. Scheidl, Adv. Phys. **49**, 607 (2000).
 - [5] D. S. Fisher, M. P. A. Fisher, and D. A. Huse, Phys. Rev. B **43**, 130 (1991).
 - [6] D. Ertas and D.R. Nelson, Physica C **272**, 79 (1996); Kierfeld, T. Nattermann and T. Hwa, Phys. Rev. B **55**, 626 (1997); T. Giamarchi and P. Le Doussal, Phys. Rev. B **55**, 6577 (1997); A.E. Koshelev and V.M. Vinokur, Phys. Rev. B **57**, 8026 (1998); B. Horowitz and T.R. Goldin, Phys. Rev. Lett. **80**, 1734, (1998); J. Kierfeld and V. Vinokur, Phys. Rev. B **61**, R14928 (2000).
 - [7] S. Ryu, A. Kapitulnik and S. Doniach, Phys. Rev. Lett. **77**, 2300 (1996); N.K. Wilkin and H.J. Jensen, Phys. Rev. Lett. **79** 4354 (1997); A. van Otterlo, R.T. Scalettar and G.T. Zimányi, Phys. Rev. Lett. **81** 1497 (1998).
 - [8] C. Reichhardt, A. van Otterlo and G.T. Zimányi, Phys. Rev. Lett. **84**, 1994 (2000).
 - [9] M.B. Gaifullin *et al.*, Phys. Rev. Lett. **84**, 2945 (2000); D. Giller *et al.*, Phys. Rev. Lett. **84**, 3698 (2000); C.J. van der Beek *et al.*, Phys. Rev. Lett. **84**, 4196 (2000).
 - [10] D. López *et al.*, Phys. Rev. Lett. **80**, 1070 (1998); A.M. Petrean *et al.*, Phys. Rev. Lett. **84**, 5852 (2000).
 - [11] Y.-H. Li and S. Teitel, Phys. Rev. Lett. **66**, 3301 (1991); T. Chen and S. Teitel, Phys. Rev. B **55**, 15197 (1997).
 - [12] X. Hu, S. Miyashita and M. Tachiki, Phys. Rev. Lett. **79**, 3498 (1997).
 - [13] Considering $dF(T, p_c(T))/dT = \partial F/\partial T + NQdp_c/dT$ for the free energies of liquid and lattice phases, and noting that along the melting line F and $E \propto \partial F/\partial T$ are equal in the two phases while the Q are not, implies that $dp_c(T)/dT = 0$.
 - [14] H. Kawamura, J. Phys. Soc. Jpn. **69**, 29 (2000).
 - [15] M. Wallin, private communication.
 - [16] Y. Nonomura and X. Hu, cond-mat/0011349.